Tetrahydrobiopterin-Free Neuronal Nitric Oxide Synthase: Evidence for Two Identical Highly Anticooperative Pteridine Binding Sites†

Antonius C. F. Gorren,‡ Barbara M. List,‡ Astrid Schrammel,‡ Eva Pitters,‡ Benjamin Hemmens,‡ Ernst R. Werner,§ Kurt Schmidt,‡ and Bernd Mayer*,‡

Institut für Pharmakologie und Toxikologie, Karl-Franzens-Universität Graz, A-8010 Graz, Austria, and Institut für Medizinische Chemie und Biochemie, Universität Innsbruck, A-6020 Innsbruck, Austria

Received August 2, 1996; Revised Manuscript Received October 25, 1996⊗

ABSTRACT: The properties of neuronal nitric oxide synthase containing one tetrahydrobiopterin (BH_4) per dimer [nNOS(BH_4+)] were compared to those of the BH_4-free enzyme [nNOS(BH_4−)]. The stimulation by BH_4 of the formation of L-citrulline at the expense of H_2O_2 production unambiguously demonstrated that BH_4 is essential in coupling reductive oxygen activation to Arg oxidation. The clear difference between the Stokes radii of nNOS(BH_4−) and nNOS(BH_4+) indicates that the introduction of one BH_4 per dimer significantly changes the enzyme structure. Whereas the heme in nNOS(BH_4+) was primarily high-spin, nNOS(BH_4−) contained mainly low-spin heme. This was slowly converted into the high-spin form with Arg and/or BH_4, with a rate that was independent of the concentration of either compound. Dithiothreitol inhibited the Arg/BH_4-induced spin conversion by stabilizing low-spin heme. Formation of high-spin heme, with rates varying from 0.04 to 0.4 min^{-1}, always correlated to an equally fast increase in activity. Radioligand binding studies showed the rapid association (within 20 s) of BH_4 to nNOS(BH_4−), but not to nNOS(BH_4+), after preincubation with Arg. Complete and monophasic dissociation of radioligand occurred in the presence of excess unlabeled BH_4, demonstrating the exchangeability of high-affinity bound BH_4. Studies of the association of N^G-nitro-L-arginine (L-NNA) to nNOS(BH_4+) revealed that excess BH_4 increased the amount of bound L-NNA 2-fold. Most of the binding data are explained by a model in which nNOS dimers accommodate two identical BH_4- and Arg/L-NNA-binding sites, with cooperativity between Arg- and BH_4-binding and anticooperativity between the BH_4-binding sites.

Nitric oxide (NO) is an important signalling and cytotoxic molecule which is synthesized by virtually all mammalian cells under certain physiological or pathophysiological conditions (Moncada et al., 1991). The functions of NO are diverse, including the regulation of vascular tone, modulation of synaptic transmission in the brain, neurotransmission in the periphery, and nonspecific immune response. NO is produced from the amino acid L-arginine by several isoforms of nitric oxide synthase (NOS)[1] [for recent reviews, see Marletta (1993), Masters (1994), Griffith and Stuehr (1995), and Mayer (1995)]. L-Arginine oxidation occurs at a cytochrome P450-like heme moiety located in the N-terminal oxygenase domain of the enzyme. The electrons required for reductive activation of molecular oxygen are shuttled in a calmodulin-dependent fashion from the donor NADPH through a FAD- and FMN-containing reductase domain to the heme. This bidomain structure of NOS suggests that it is a fusion protein of a cytochrome P450 and a P450 reductase, resembling the bacterial cytochrome $P450_{BM-3}$ (Fulco, 1991; Degtyarenko & Archakov, 1993).

In contrast to all other cytochrome P450s, NOS requires the pteridine derivative (6*R*)-5,6,7,8-tetrahydro-L-biopterin (tetrahydrobiopterin, BH_4) as an additonal cofactor (Mayer & Werner, 1995). The function of BH_4 in NO biosynthesis shows fundamental differences compared to the well-established role of the pteridine as a cofactor of aromatic amino acid hydroxylases (Kaufman, 1993). While the latter enzymes are non-heme iron proteins utilizing free BH_4 as a hydroxylating species, NOS contains BH_4 as a tightly associated prosthetic group which does not undergo net oxidation during catalysis. Thus, if it is indeed participating as a redox-active cofactor in L-arginine oxidation, BH_4 must be continuously recycled by an intrinsic dihydropteridine reductase activity of NOS (Mayer et al., 1991; Witteveen et al., 1996). In addition to this putative function of BH_4 as a redox-active cofactor, the pteridine may be essential in promoting the assembly of NOS subunits to form active homodimers. However, whereas dimerization of inducible NOS (iNOS) shows an absolute requirement for both heme and BH_4 (Baek et al., 1993; Tzeng et al., 1995), dimerization of the constitutively expressed neuronal isoform (nNOS) appears to be pteridine-independent and regulated solely by the availability of heme (Klatt et al., 1996). Although partially BH_4-deficient homodimeric nNOS is able to catalyze the reduction of molecular oxygen (Mayer et al., 1991;

† This work was supported by Grants P 11478, P 10655, P 11859 (B.M.), P 10573 (K.S.), and P 11301 (E.R.W.) of the Fonds zur Förderung der Wissenschaftlichen Forschung in Österreich.

* Corresponding author: Institut für Pharmakologie und Toxikologie, Karl-Franzens-Universität Graz, Universitätsplatz 2, A-8010 Graz, Austria. Telephone: 43-316-380-5567. Fax: 43-316-380-9890. E-mail: mayer@kfunigraz.ac.at.

‡ Karl-Franzens-Universität Graz.

§ Universität Innsbruck.

⊗ Abstract published in *Advance ACS Abstracts,* December 1, 1996.

[1] Abbreviations: NOS, nitric oxide synthase; nNOS, iNOS, and eNOS, neuronal, inducible, and endothelial isoforms of NOS, respectively; BH_4, (6*R*)-5,6,7,8-tetrahydro-L-biopterin (tetrahydrobiopterin); nNOS(BH_4+) and nNOS(BH_4−), nNOS containing approximately 1 equiv of BH_4 per dimer and BH_4-free nNOS, respectively; DAHP, 2,4-diamino-6-hydroxypyrimidine; L-NNA, N^G-nitro-L-arginine; CHAPS, 3-[(3-cholamidopropyl)dimethylammonio]-1-propanesulfonate; DTT, dithiothreitol.

S0006-2960(96)01931-9 CCC: $12.00

Heinzel et al., 1992), it does not exhibit NOS activity unless converted into a tight, superstable dimer by saturation with exogenous BH_4 (Klatt et al., 1995). One of the key problems in understanding the function of BH_4 in nNOS seems to us to be the peculiar stoichiometry of BH_4 binding to the homodimeric enzyme. Recently, we have overexpressed nNOS in Sf9 cells under different conditions of infection, yielding preparations with varying amounts of endogenous heme (List et al., 1996). This study revealed that nNOS always contained heme and BH_4 in a ratio of 2:1, with each dimer containing two hemes and one tightly bound BH_4 at most. Notwithstanding, dimers apparently half-saturated with BH_4 were stimulated 2-fold in the presence of the exogenously added cofactor, clearly suggesting that the enzyme is able to bind two BH_4 molecules per dimer (List et al., 1996).

The present study was carried out to elucidate the intriguing binding characteristics of BH_4 using an essentially BH_4-free preparation of nNOS. Since the endogenous pteridine of conventional enzyme preparations proved to be inaccessible to antagonists of BH_4 binding (Klatt et al., 1994a), we set out to overexpress a BH_4-deficient form of the protein in Sf9 cells under conditions of reduced pteridine availability. Expression in insect cells treated for prolonged periods with high concentrations of 2,4-diamino-6-hydroxypyrimidine (DAHP), an inhibitor of GTP cyclohydrolase I, yielded a functionally intact dimeric nNOS species, which we have characterized with respect to its structural and optical features, as well as regarding its BH_4 binding properties.

MATERIALS AND METHODS

Materials. Purified recombinant rat nNOS was obtained from baculovirus-infected insect cells as described previously (Harteneck et al., 1994; Mayer et al., 1996). For expression of BH_4-deficient nNOS, Sf9 cells were preincubated for 24 h with 10 mM DAHP followed by infection with the recombinant baculovirus for 48 h in the presence of DAHP. The protocol for enzyme purification was the same as applied for control preparations. L-[2,3,4,5-^{3}H]Arginine hydrochloride (57 Ci/mmol) and N^G-nitro-L-[2,3,4,5-^{3}H]arginine hydrochloride (L-[^{3}H]NNA, 56 Ci/mmol) were purchased from MedPro (Amersham, Vienna, Austria). [3′-^{3}H]-(6*R*)-5,6,7,8-Tetrahydro-L-biopterin ([^{3}H]BH_4) was synthesized as described previously (Werner et al., 1994).

Determination of Cofactors and Enzyme Activities. Enzyme-bound heme, FAD, FMN, and BH_4 were determined by HPLC and UV/vis- or fluorescence detection as previously described (Mayer et al., 1996). Values are expressed as moles of cofactor per mole of 160 kDa subunit (equivalents per subunit) on the basis of protein determination with the Bradford method using bovine serum albumin as a standard (Bradford, 1976). Likewise, nNOS concentrations are expressed as the concentration of the monomer, assuming a molecular mass of 160 000 Da.

NOS activity was determined as the formation of L-[2,3,4,5-^{3}H]citrulline from L-[2,3,4,5-^{3}H]arginine (Mayer et al., 1994). Unless otherwise indicated, 0.2−0.3 μg enzyme (1.3−1.9 pmol) was incubated in a final volume of 0.1 mL at 37 °C for 10 min in 50 mM triethanolamine/HCl (pH 7.0) containing 0.1 mM [^{3}H]arginine (∼50000 cpm), 0.2 mM NADPH, 5 μM FAD, 5 μM FMN, 10 μM BH_4, 0.5 mM $CaCl_2$, 10 μg/mL calmodulin, and 0.2 mM CHAPS (Klatt et al., 1996), followed by separation and detection of [^{3}H]citrulline. In those experiments, in which the correlation between the time-dependent spectral changes, induced by the addition of BH_4 and/or Arg to nNOS(BH_4−) on the one hand, and the change in the specific activity on the other was investigated (*vide infra*), the incubation time in the activity assays was limited to 2 min instead of 10 min, and the enzyme concentration was 5 times higher [0.75 μg (4.7 pmol) of nNOS].

Generation of H_2O_2 was determined spectrophotometrically as previously described (Heinzel et al., 1992). Purified nNOS (1.5 μg, 9.4 pmol) was incubated at 37 °C for 10 min in a final volume of 0.2 mL of a 50 mM triethanolamine/HCl buffer (pH 7.0) in the presence of 0.1 mM Arg, 0.5 mM $CaCl_2$, 0.4 mM NADPH, 1 μM FAD, 1 μM FMN, 10 μg/mL calmodulin, and increasing concentrations of BH_4 (10^{-9}−10^{-4} M). Following addition of 100 μL of concentrated HCl, 20 μL of $Fe(NH_4)_2(SO_4)_2$ (56 mM), and 30 μL of KSCN (2.1 M), the absorbance at 492 nm was measured against calmodulin-deficient blanks. The rates of H_2O_2 formation were calculated from calibration curves recorded with solutions of authentic H_2O_2 that had undergone the same procedure.

Gel Filtration Chromatography. Purified nNOS (0.2 mL, 0.15−0.20 mg) was injected onto a HPLC system (LiChro Graph L=6200, Merck) equipped with a low-pressure gradient controller and a gel filtration column (Superose 6, HR 10/30, Pharmacia, Biotech, Vienna, Austria) providing a separation range from approximately 5 to 5000 kDa. The column was calibrated with the gel filtration calibration kit from Pharmacia Biotech, including Blue Dextrane 2000 (determination of the void volume), thyroglobulin (669 kDa, Stokes radius = 8.50 nm), ferritin (440 kDa, 6.10 nm), catalase (232 kDa, 5.22 nm), aldolase (158 kDa, 4.81 nm), and bovine serum albumin (67 kDa, 3.55 nm) in 50 mM triethanolamine/HCl (pH 7.0) containing 0.5 mM EDTA and 500 mM NaCl at a flow rate of 0.3 mL/min at room temperature. Calibration curves were obtained by plotting $(-\log K_{av})^{0.5}$ against the Stokes radii of the standard proteins [$K_{av} = (V_e V_0)/(V_t - V_0)$, with V_e, V_0, and V_t denoting the elution volume of the protein, the column void volume, and the total bed volume of the column].

Light Absorbance Spectroscopy. Absorbance spectra were measured with a Hewlett-Packard 8452A diode array spectrophotometer. For absorbance measurements, nNOS samples were diluted to a final concentration of approximately 5 μM. As a result, for all optical experiments, a concentration between 3 and 6 mM β-mercaptoethanol must be taken into account, since the concentrations of the nNOS(BH_4+) and -(BH_4−) preparations we used varied between 10 and 20 μM and since the nNOS preparations were stored in a buffer containing 20 mM Tris (pH 7.0), 150 mM NaCl, 4 mM EGTA, and 12 mM β-mercaptoethanol.

Radioligand Binding Studies. Radioligand binding experiments were performed as described previously (Klatt et al., 1994a,b). For association kinetics, purified nNOS (60 μg, 375 pmol) was incubated at 37 °C with [^{3}H]BH_4 (7−10 nM) or L-[^{3}H]NNA (11−12 nM) in 2 mL of a 50 mM triethanolamine/HCl buffer (pH 7.0). At the indicated time points, 0.1 mL aliquots were removed from the incubation mixture and assayed for bound [^{3}H]BH_4 or L-[^{3}H]NNA. For dissociation kinetics, the same procedure was followed, except that after 10 min of incubation of the enzyme with the radioligand a large excess (1 mM) of the corresponding

unlabeled compounds was added. At the indicated time points, 0.1 mL aliquots were removed and assayed for specifically bound radioligands. Whenever indicated, the enzyme preparations were preincubated for 30 min at ambient temperature with 0.1 mM Arg ([^{3}H]BH_4 binding) or 10 μM BH_4 (L-[^{3}H]NNA binding) prior to addition of the radiolabels. Rate constants were calculated by fitting the individual data according to pseudo-first-order (association) or first-order (dissociation) kinetics.

RESULTS

Cofactor Content of BH_4-Deficient nNOS. We have previously reported that virtually BH_4-free nNOS can be obtained from baculovirus-infected Sf9 cells under conditions of reduced BH_4 availability (List et al., 1996). To this goal, Sf9 cells were incubated with the GTP cyclohydrolase I inhibitor DAHP (10 mM) for 24 h before as well as during infection. DAHP had no apparent effect on cell viability. Using a standard purification procedure (Mayer et al., 1996), we obtained about 50 mg of an electrophoretically homogeneous 160 kDa protein from 4.5×10^9 cells (3 L cultures). The purified enzyme contained stoichiometric amounts of heme (0.91 ± 0.09) and 0.4−0.5 equiv of FAD and FMN per subunit. These values are identical to previous data obtained with the enzyme expressed under control conditions (Harteneck et al., 1994; List et al., 1996), showing that DAHP had no effect on binding of the heme or the flavins to nNOS. However, there was a pronounced effect of the inhibitor on the amount of bound BH_4; whereas the maximal BH_4 content in isolated nNOS is 0.5 equiv per subunit (List et al., 1996), expression of the protein in the presence of DAHP reduced this value to 0.06 ± 0.02. Throughout this paper, this virtually BH_4-free preparation will be designated as nNOS(BH_4−) and the control preparation containing ∼0.5 equiv of BH_4 per subunit as nNOS(BH_4+).

Enzymatic Activity of BH_4-Deficient nNOS. The pteridine-deficient enzyme exhibited only marginal activity (∼0.06 μmol of L-citrulline·mg^{-1}·min^{-1}) but was stimulated about 10-fold by the addition of BH_4 (0.59 ± 0.05 μmol·mg^{-1}·min^{-1}). Nevertheless, the activity of nNOS(BH_4−), determined under standard assay conditions, was always lower than that of nNOS(BH_4+) (0.8−1.0 μmol·mg^{-1}·min^{-1}).

Previous studies with purified porcine nNOS indicated that a lack of BH_4 leads to uncoupling of reductive oxygen activation even in the presence of saturating concentrations of Arg (Heinzel et al., 1992; Klatt et al., 1993). The availability of virtually BH_4-free recombinant nNOS allowed us to unequivocally settle this issue. Figure 1 shows the concentration-dependent effect of BH_4 on the formation of L-citrulline and H_2O_2, a marker for the uncoupling of NADPH oxidation from L-arginine metabolism. Despite the presence of 0.1 mM Arg, in the absence of BH_4, the enzyme produced virtually no L-citrulline and showed considerable uncoupling of NADPH oxidation as revealed by the formation of H_2O_2 at a rate of 0.5 μmol·mg^{-1}·min^{-1}. Increasing concentrations of BH_4 stimulated L-citrulline formation to a maximal specific activity of about 0.5 μmol·mg^{-1}·min^{-1} and equivalently lowered the enzymatic H_2O_2 production. The BH_4 concentration producing half-maximal effects was identical for both reactions (∼0.2 μM), demonstrating that coupling of reductive oxygen activation to L-arginine oxidation requires the presence of BH_4.

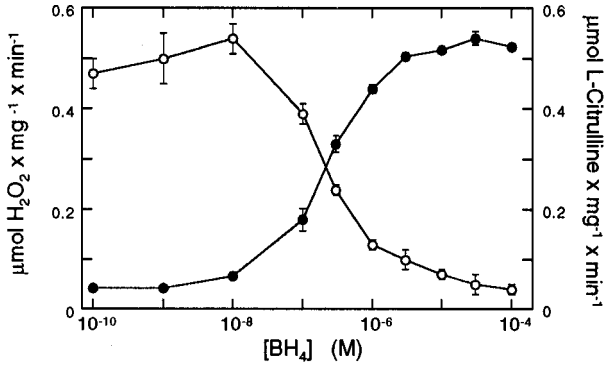

FIGURE 1: Effect of BH_4 on the formation of L-citrulline and H_2O_2 by nNOS(BH_4−). Rates of formation of H_2O_2 (open circles) and L-citrulline (closed circles) were determined as described in Materials and Methods and are given as the mean values of three experiments. Experimental conditions were as follows: 12−19 nM (L-citrulline formation) or 47 nM (H_2O_2 formation) nNOS(BH_4−), 50 mM triethanolamine/HCl (pH 7.0), 100 μM L-arginine, 400 μM NADPH, 10 μg/mL calmodulin, 500 μM $CaCl_2$, and 1 μM (H_2O_2 formation) or 5 μM (L-citrulline formation) FMN/FAD.

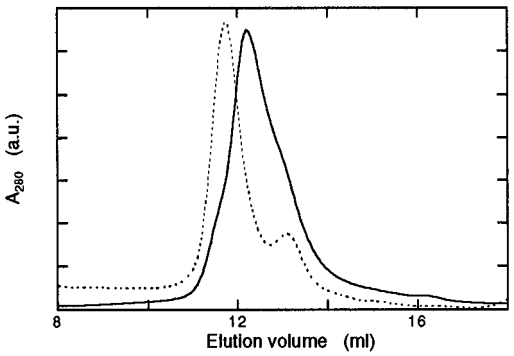

FIGURE 2: Gel filtration chromatography of nNOS(BH_4−). The elution profile of the enzyme as isolated is shown by a continuous line. The dashed line is the elution profile obtained after preincubation with 200 μM BH_4 and 1 mM Arg for 30 min at room temperature and 5 min at 37 °C and with 1 mM Arg in the elution buffer. See Materials and Methods for experimental details.

Stokes Radius of BH_4-Deficient nNOS. To investigate the effect of BH_4 deficiency on protein structure, we determined the Stokes radius of nNOS(BH_4−) by gel filtration chromatography. In agreement with previous studies (Klatt et al., 1995, 1996), the nNOS(BH_4+) dimer eluted after 11.62 ± 0.06 mL, yielding a Stokes radius of 8.5 ± 0.1 nm, whereas the monomer, present as a small fraction, eluted after 12.99 ± 0.06 mL, yielding a Stokes radius of 6.6 ± 0.1 nm. These values were not changed by preincubation and chromatography of the protein in the presence of 10 μM BH_4 and/or 0.1 mM Arg (not shown). In the case of nNOS(BH_4−), the main band eluted after 12.32 ± 0.05 mL, yielding a Stokes radius of 7.5 ± 0.1 nm, distinctly different from that of both dimeric and monomeric nNOS(BH_4+) (Figure 2). In the presence of BH_4 and/or Arg, the chromatogram of nNOS(BH_4−) resembled that of nNOS(BH_4+), with Stokes radii of 8.3 ± 0.1 nm and 6.6 ± 0.1 nm for the dimer and monomer, respectively. These results indicate that there are significant structural differences between nNOS(BH_4+) (containing 0.5 equiv of BH_4 per monomer) and nNOS(BH_4−), whereas complete pteridine saturation had no apparent further effect. Since the radius of nNOS(BH_4−) was considerably larger than that of monomeric nNOS (6.3 nm; Klatt et al., 1996), the pteridine-free protein was probably dimeric, with the difference between nNOS(BH_4+)

Table 1: Observed Kinetic Parameters for the Binding of BH_4 to nNOS[a]

		association[b]				dissociation[c]		calculated constants	
enzyme	Arg (100 μM)	v_{on} (nM·min^{-1})	[[^{3}H]BH_4]$_0$ (nM)	Δ[[^{3}H]BH_4] (nM)	k_{obs} (min^{-1})	k_{off}[d] (min^{-1})	[[^{3}H]BH_4]$_0$ (nM)	k_{on}[e] (μM^{-1}·min^{-1})	v_{on}^{calc}[f] (nM·min^{-1})
nNOS(BH_4−)	−	0.141 ± 0.008	0.05 ±0.02	0.52 ±0.05	0.6 ±0.3	0.16 ±0.04	0.30 ±0.01	0.7	0.9
	+	0.15 ±0.02	1.6 ±0.2	0.7 ±0.2	0.6 ±0.3	0.070 ±0.006	1.9 ±0.1	1.9	2.5
nNOS(BH_4+)	−	0.17 ±0.01	0.14 ±0.04	0.88 ±0.04	0.41 ±0.09	0.28 ±0.02	1.14 ±0.03	1.2	2.0
	+	0.23 ±0.04	0.5 ±0.1	1.9 ±0.1	0.14 ±0.05	0.067 ±0.005	2.2 ±0.1	1.8	2.9

[a] Association and dissociation rates of radiolabeled BH_4 were determined as described in Materials and Methods. The concentration of nNOS was 187.5 nM; the concentrations of [^{3}H]BH_4 were 7.0 and 8.7 nM in the experiments with nNOS(BH_4−) and nNOS(BH_4+), respectively. Reactions were carried out at 37 °C in 50 mM triethanolamine/HCl buffer (pH 7.0). Where indicated, preincubation with 100 μM Arg was performed for 30 min at ambient temperature. Dissociation was initiated by the addition of 1 mM unlabeled BH_4. All values are averages of three experiments. [b] Fitted both to zero- and first-order kinetics. v_{on} is the observed zero-order binding rate. [[^{3}H]BH_4]$_0$ was obtained by extrapolating linear fits to zero time and represents the concentration of rapidly binding pteridine; Δ[[^{3}H]BH_4] is the concentration of [^{3}H]BH_4 bound during incubation and represents the slow-binding pteridine. k_{obs} is the observed first-order binding rate constant. Zero-order kinetics gave superior fits in all cases. [c] Fitted assuming first-order kinetics, with k_{off} and [[^{3}H]BH_4]$_0$ representing the dissociation rate constant and the concentration of bound [^{3}H]BH_4 at zero time, respectively. [d] The rates observed without Arg [0.16 and 0.34 min^{-1} for nNOS(BH_4−) and nNOS(BH_4+), respectively] were corrected for the apparent dissociation rate observed in the absence of unlabeled BH_4, by subtracting 0.07 min^{-1}. [e] Calculated with the published values of the dissociation constant of BH_4 for nNOS in the absence and presence of Arg (230 and 37 nM, respectively; Klatt et al., 1994a), and the observed dissociation rate constants according to $k_{on} = k_{off}/K_d$. [f] Initial rate; calculated with the equation $v_{on}^{calc} = k_{on}$[[^{3}H]BH_4][nNOS].

and nNOS(BH_4−) resulting from a change in protein conformation.

BH_4 Binding to and Dissociation from nNOS. The intriguing fact that nNOS maximally contains one tightly bound BH_4 molecule per dimer but doubles its activity upon binding of a second molecule led us to suggest that the dimeric enzyme may exhibit two distinct pteridine sites (List et al., 1996). Interpretation of radioligand binding studies on this topic is complicated by the endogenous BH_4 already present in nNOS(BH_4+) (Klatt et al., 1994a). Thus, the kinetics of BH_4 binding to nNOS(BH_4−) were studied and compared to those of nNOS(BH_4+), both with and without preincubation in the presence of Arg, with a special emphasis on the possible detection of a second pteridine binding site. From these studies, apparent association and dissociation rate constants that are quite similar to those published previously for nNOS(BH_4+) can be calculated (Table 1). However, on closer examination, the results take on a far more complex appearance.

Preincubation with Arg of either nNOS(BH_4−) or nNOS(BH_4+) had no obvious effect on the BH_4 association rate but caused a considerable increase of the final levels of bound [^{3}H]BH_4 (Figure 3A). In the absence of Arg, the final [^{3}H]BH_4 concentrations were 0.6 ± 0.1 and 1.0 ± 0.1 nM for nNOS(BH_4−) and nNOS(BH_4+), respectively; the corresponding values in the presence of Arg were 2.3 ± 0.2 and 2.4 ± 0.1 nM. The most prominent difference between the two enzyme forms nNOS(BH_4−) and nNOS(BH_4+) existed in the association of BH_4 after preincubation of the enzyme with arginine (Figure 3A). The final concentration of bound [^{3}H]BH_4 was similar for both enzymes; however, with nNOS(BH_4−), most of the reaction (1.6 ± 0.2 nM, 70%) occurred rapidly (within the first 20 s), whereas with nNOS(BH_4+), the fast-reacting BH_4 fraction was much smaller (0.5 ± 0.1 nM, 21%) (Table 1). In the absence of Arg, the rapidly reacting fractions were insignificant for either enzyme form (Figure 3A). Although a complete interpretation still poses some problems (see Discussion), these results provide the first unequivocal evidence of two distinct BH_4 binding modes in nNOS. BH_4 can only bind rapidly to the BH_4-free enzyme in the presence of Arg. When this high-affinity binding site is already occupied, as in nNOS(BH_4+), BH_4 association is much slower.

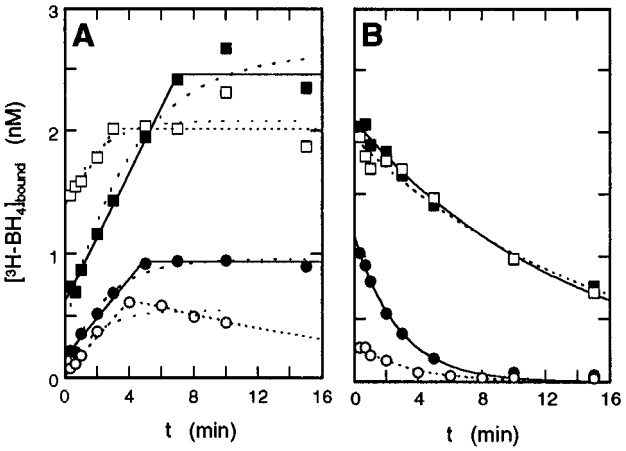

FIGURE 3: Kinetics of BH_4 binding. (A) Association of BH_4 to nNOS. Radiolabeled BH_4 was added to nNOS(BH_4−) (open symbols, dashed lines) or nNOS(BH_4+) (closed symbols, continuous lines), and the binding was monitored as described in Materials and Methods. Prior to the binding experiments, nNOS was preincubated for 30 min in the absence (circles) or presence (squares) of 100 μM L-arginine at room temperature. Experimental conditions were as follows: 187.5 nM nNOS, 7.0−9.2 nM [^{3}H]-BH_4, 50 mM triethanolamine/HCl (pH 7.0), and 37 °C. (B) Dissociation of BH_4 from nNOS. The release of radiolabeled BH_4 from nNOS(BH_4−) or nNOS(BH_4+) in the presence of a large excess (1 mM) of unlabeled BH_4 was determined as described in Materials and Methods. The symbols have the same meaning as in panel A. All plots are representative of three experiments. The data points in panel A were fitted to a straight line as well as to a single exponential [pseudo-first-order kinetics; dotted lines; $c_t = c_0 + \Delta c[1 - \exp(-kt)]$, in which c_0 and Δc are the concentrations of rapidly and slowly bound radioligand, respectively, and k is the observed pseudo-first-order rate constant]. Data points in panel B were fitted to a single exponential [first-order kinetics; $c_t = c_0 \exp(-kt)$]. The kinetic parameters, obtained from the fits, are incorporated in Table 1.

There is yet another aspect to the BH_4 association that needs to be addressed. Although the data could be fitted to an exponential curve, in line with the expected pseudo-first-order behavior, the fits, at least for the experiments performed in the presence of arginine, were rather inadequate, and a considerably better fit was obtained assuming a linear relationship, indicative of a (pseudo-) zero-order reaction (Figure 3A). This prompted us to take a closer look at the

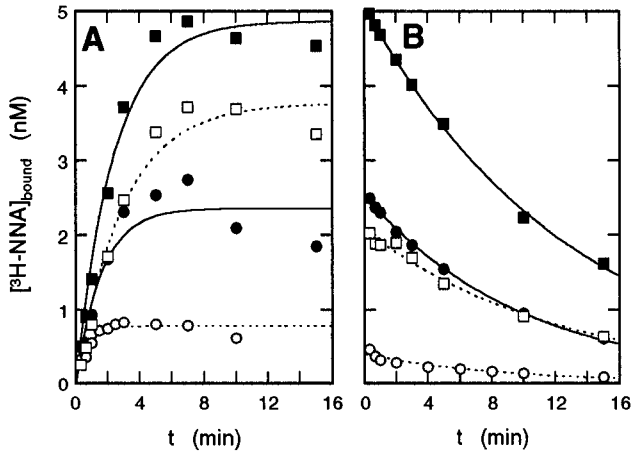

FIGURE 4: Kinetics of L-NNA binding. (A) Association of L-NNA to nNOS. L-[^{3}H]NNA was added to nNOS(BH_4−) (open symbols, dashed lines) or nNOS(BH_4+) (closed symbols, continuous lines), and the binding was monitored as described in Materials and Methods. Prior to the binding experiments, nNOS was preincubated for 30 min in the absence (circles) or presence (squares) of 10 μM BH_4 at room temperature. Experimental conditions were as follows: 187.5 nM nNOS, 11.7−11.9 nM L-[^{3}H]NNA, 50 mM triethanolamine/HCl (pH 7.0), and 37 °C. (B) Dissociation of L-NNA from nNOS. The release of L-[^{3}H]NNA from nNOS(BH_4−) or nNOS(BH_4+) in the presence of a large excess (1 mM) of unlabeled L-NNA was determined as described in Materials and Methods. The symbols have the same meaning as in panel A. All plots are representative of three experiments. The data points in panel A were fitted to a single exponential [pseudo-first-order kinetics; $c_t = \Delta c[1 - \exp(-kt)]$, in which Δc represents the concentration of bound radioligand and k is the observed first-order rate constant]. Data points in panel B were fitted to a single exponential [first-order kinetics; $c_t = c_0 \exp(-kt)$, in which c_0 represents the concentration of radioligand bound at $t = 0$]. The kinetic parameters, obtained from the fits, are incorporated in Table 2.

concentration dependence of the association of BH_4 to Arg-preincubated nNOS(BH_4+). The binding rate was linearly dependent on the enzyme concentration, but, in accordance with the apparent zero-order behavior, independent of the concentration of BH_4 (not shown).

The dissociation of BH_4 from nNOS, as determined from the displacement of [^{3}H]BH_4 by unlabeled BH_4, appeared to be more straightforward. Almost identical curves were obtained for both nNOS(BH_4−) and nNOS(BH_4+) that had been preincubated with Arg (Figure 3B). In both cases, the results could be fitted to a single exponential with very similar rate constants (Table 1). When Arg had been omitted during preincubation, far higher rate constants were observed (Figure 3B). Control experiments performed without unlabeled BH_4 showed virtually no decay ($\leq$0.01 min^{-1}) for enzyme preincubated with Arg and a relatively slow decay (0.065 ± 0.005 min^{-1}) in the absence of Arg (not shown).

N^G-Nitro-L-arginine Binding to and Dissociation from nNOS. Binding of the inconvertible substrate analogue N^G-nitro-L-arginine (L-NNA) was shown to be stimulated 2-fold by the addition of BH_4 to nNOS(BH_4+) (Klatt et al., 1994a). With this in mind, and taking into account the complexities of BH_4 binding reported above, we decided to investigate the binding of L-NNA to nNOS(BH_4+) and nNOS(BH_4−) more closely. The main effect of BH_4 on the association of L-NNA to nNOS was on the final concentration of bound L-[^{3}H]NNA (Figure 4A). In the presence of additional BH_4, twice as much L-[^{3}H]NNA (4.7 ± 0.2 nM) was bound to nNOS(BH_4+) than in the absence of BH_4 (2.4 ± 0.4 nM) (Table 2). Very little L-[^{3}H]NNA (0.8 ± 0.3 nM) was bound to nNOS(BH_4−), unless BH_4 was present, in which case the concentration of bound L-[^{3}H]NNA (3.5 ± 0.3 nM) approached that obtained with nNOS(BH_4+). These combined results suggest a strong correlation between BH_4 and L-NNA binding, in that L-NNA binding only occurs to NOS that has already bound BH_4. At the same time, the doubling of the level of L-NNA bound to nNOS(BH_4+) after preincubation with BH_4 as well as the conspicuous lack of binding of L-NNA to nNOS(BH_4−) in the absence of BH_4 provide the most direct evidence thus far for the presence on nNOS of two BH_4 binding sites.

In contrast to the striking effects of BH_4 on the amount of L-NNA that bound to nNOS, the effects of BH_4 on the rate of binding were ambiguous (Table 2). If anything, BH_4 appeared to lower the pseudo-first-order association rate constant. Unlike the association rate of BH_4, the association rate of L-NNA was linearly dependent on the L-NNA concentration (not shown). The dissociation, as determined from the displacement of L-[^{3}H]NNA by unlabeled L-NNA, proceeded similarly in all cases, except for the different starting concentrations (Figure 4B). All curves could be fitted to single exponentials with rate constants between 0.08 and 0.10 min^{-1} (Table 2).

Absorbance Spectrum of nNOS(BH_4−). The absorbance spectrum of nNOS(BH_4−) differed strongly from that of native nNOS(BH_4+). The Soret region was characterized by a peak at 418 nm and shoulders at 380−400 and at 455 nm, whereas at higher wavelengths, weak bands at 540−580 and at 650 nm could be discerned (Figure 5A). Addition of 1 mM dithiothreitol (DTT) caused the instantaneous appearance of a spectrum with two strong Soret bands at 378 and 458 nm and weak shoulders at 550 and 580 nm. A spectrum very similar to that observed in the presence of DTT could also be obtained by the addition of β-mercaptoethanol; however, a much higher concentration (50 mM) was required, and a residual band at 416 nm remained visible (not shown).

BH_4- and L-Arginine-Induced Absorbance Changes. When 10 μM BH_4 was added to nNOS(BH_4−), a spectrum was obtained that was nearly identical to that of nNOS(BH_4+), with a Soret peak at 396 nm, a weak shoulder at 455 nm and a stronger one at 480 nm, and bands in the α and β regions at 545 and 650 nm (Figure 5A). The absorbance difference spectrum exhibited maxima at 395, 486, and 655 nm and minima at 424, 456, and 570 nm. The transition was not monophasic; the absorbance increase at 398 nm took place primarily in the first 10 min. Upon longer incubation, little further increase occurred at 398 nm and a maximum at 480 nm became apparent (Figure 5B). Other maxima at that stage in the reaction were observed at 330 and 605 nm, while the main mininum was at 419 nm.

Very similar observations were made when, instead of BH_4, Arg (200 μM) was added to nNOS(BH_4−) (not shown). Absorbance decreases at 426, 455, and 575 nm were accompanied by increases at 395, 500, and 655 nm and, upon longer incubation, by an increase at 480 nm, although the latter effect was usually less prominent than with BH_4. Addition of BH_4 to Arg-preincubated nNOS(BH_4−), or of Arg to BH_4-preincubated nNOS(BH_4−), did not induce any further significant absorbance changes. Simultaneous addition of BH_4 and Arg had the same effect as the addition of either compound alone.

Table 2: Observed Kinetic Parameters for the Binding of L-NNA to nNOS[a]

		association[b]		dissociation[c]		calculated parameters	
enzyme	BH_4 (10 μM)	k_{obs} (min^{-1})	Δ[[^{3}H]NNA] (nM)	k_{off} (min^{-1})	[[^{3}H]NNA]$_0$ (nM)	k_{on}[d] ($\mu M^{-1}\cdot min^{-1}$)	K_d[e] (nM)
nNOS(BH_4-)	−	1.4 ± 0.9	0.8 ± 0.3	0.10 ± 0.02	0.34 ± 0.08	7 ± 5	20 ± 30
	+	0.38 ± 0.08	3.5 ± 0.3	0.083 ± 0.008	1.98 ± 0.07	1.6 ± 0.5	50 ± 30
nNOS(BH_4+)	−	0.6 ± 0.2	2.4 ± 0.4	0.097 ± 0.002	2.54 ± 0.02	3 ± 1	30 ± 20
	+	0.38 ± 0.06	4.7 ± 0.2	0.079 ± 0.004	5.03 ± 0.07	1.6 ± 0.3	50 ± 10

[a] Association and dissociation rates of radiolabeled L-NNA were determined as described in Materials and Methods. The concentration of nNOS was 187.5 nM; the concentrations of L-[^{3}H]NNA were 11.7 and 11.9 nM in the experiments with nNOS(BH_4-) and nNOS(BH_4+), respectively. Reactions were carried out at 37 °C in 50 mM triethanolamine/HCl buffer (pH 7.0). Where indicated, preincubation with 10 μM BH_4 was performed for 30 min at ambient temperature. Dissociation was initiated by the addition of 1 mM unlabeled L-NNA. All values are averages of three experiments. [b] Fitted assuming pseudo-first-order kinetics; k_{obs} is the observed binding rate constant and Δ[[^{3}H]NNA] the corresponding concentration of bound L-[^{3}H]NNA. [c] Fitted assuming first-order kinetics; k_{off} is the observed dissociation rate constant and [[^{3}H]NNA]$_0$ the concentration of bound L-[^{3}H]NNA at zero time. [d] Calculated according to $k_{on} = (k_{obs} - k_{off})/[nNOS]$. [e] Calculated according to $K_d = k_{off}/k_{on}$.

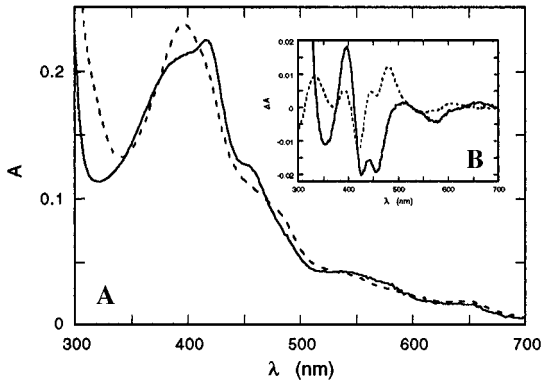

FIGURE 5: Optical absorbance spectrum of nNOS(BH_4-) and the effect of BH_4. (A) Absorbance spectra of nNOS(BH_4-) were recorded in the absence (continuous line) and presence (dashed line) of BH_4. (B) Absorbance difference spectra of the changes induced by BH_4 in the first 10 min after addition (continuous line) and in the interval from 10 to 90 min after addition (dashed line). Experimental conditions were as follows: 4.7 μM nNOS(BH_4-), 10 μM BH_4, 50 mM triethanolamine/HCl (pH 7.0), and 25 °C.

The kinetics of the absorbance changes induced by BH_4 and/or Arg were biphasic. Similar rates were obtained with BH_4 and Arg. The faster phase, which corresponded to the absorbance increase at 398 nm, proceeded with observed first-order rate constants of 0.47 ± 0.01 and 0.59 ± 0.09 min^{-1} for BH_4 and Arg, respectively. The rate constants of the slower phase, characterized by the absorbance maximum at 480 nm, were 0.108 ± 0.006 and 0.128 ± 0.005 min^{-1}. Both the rates and the amplitudes of the two phases were independent of the concentration of either compound (between 10 and 60 μM BH_4 and 100 and 500 μM Arg). Very small absorbance changes, resembling those observed with nNOS(BH_4-), were also observed after the addition of Arg or BH_4 to nNOS(BH_4+).

When Arg (200 μM) was added to nNOS(BH_4-) in the presence of 1 mM DTT, a transition to the spectrum of native NOS was again observed, but with an appreciably diminished rate (Table 3). When the same reaction was carried out in the presence of 10 mM DTT, the rate became lower still, and the transition was incomplete. Increasing the Arg concentration hardly affected the rate of the transition but significantly enhanced the amplitude of the absorbance change. Similar results were obtained with BH_4 instead of Arg (Table 3), except that, at least for BH_4 concentrations upward of 10 μM, a complete transition was always observed (not shown).

Correlation between Activity and Spectral Changes. To establish whether the spectral changes induced by either Arg or BH_4 correlate with the specific activity of nNOS, aliquots were taken from the absorbance samples at various times and assayed for L-citrulline production under standard conditions, except that the incubation period was 2 rather than 10 min and 5 times the usual enzyme concentration was applied (see Materials and Methods). Figure 6A shows the effect of Arg incubation on both the nNOS(BH_4-) absorbance and the specific activity. An excellent correlation was found between the first spectral phase (k_{app} = 0.22 min^{-1}) and an increase in specific activity, whereas no further increase in activity was observed during the slower spectral phase. Similarly, the faster spectral phase observed in the presence of 10 μM BH_4 (k_{app} = 0.26 min^{-1}), but not the slower one, correlated with an increase in L-citrulline production (Figure 6B).

The correlation between the spectral changes and the specific activity was further corroborated by performing similar experiments with enzyme preincubated with 1 mM DTT. Again, the considerably slower, in this case, spectral changes were mirrored by an increase in activity proceeding at an equally reduced rate (Figure 6C). Remarkably, the final activity obtained in this experiment was somewhat higher than that observed when preincubation was carried out in the absence of DTT and approached the activity of nNOS(BH_4+). The same strong correlation was also observed with 500 μM Arg and 10 mM DTT, both between the rates and the amplitudes of the absorbance and activity changes (Table 3).

Very small absorbance changes of varying amplitude, resembling those observed after the addition of Arg or BH_4, were usually observed when nNOS(BH_4-) was incubated (at 25 °C) in the absence of added ligands. These absorbance changes correlated with an equally small increase in activity. When, after preincubation at 25 °C for 25 min, Arg (100 μM) was added, both the spectral changes and the rise in activity were again observed (not shown). Preincubation of nNOS(BH_4+) at 25 °C affected neither the activity nor the absorbance. Addition of Arg after 25 min induced a small absorbance change, with a concomitant small increase in the specific activity (not shown).

DISCUSSION

Effect of BH_4 Depletion on Cofactor Content, Structure, Quaternary Structure, and Enzyme Activity of nNOS

We have previously reported on expression and purification of nNOS highly deficient in BH_4 but otherwise quite similar to the native enzyme (List et al., 1996). The results

Table 3: Effects of BH_4, L-Arginine, and DTT on the Absorbance Spectrum and the Specific Activity of nNOS(BH_4−)[a]

added compounds[b]			absorbance[c]			specific activity[d]		
BH_4 (μM)	L-Arg (μM)	DTT (mM)	k_{obs} (min^{-1})	ΔA	$10^4\alpha$ (min^{-1})	k_{obs} (min^{-1})	Δact. (nmol·mg^{-1}·min^{-1})	act.$_0$ (nmol·mg^{-1}·min^{-1})
10	−	−	0.26 ± 0.02	0.041 ± 0.002	1.9 ± 0.4	0.3 ± 0.1	430 ± 70	200 ± 80
−	200	−	0.22 ± 0.04	0.055 ± 0.004	2.2 ± 0.6	0.18 ± 0.07	570 ± 80	170 ± 70
−	200	1	0.15 ± 0.03[e]	0.067 ± 0.009	4 ± 1	0.10 ± 0.05[f]	630 ± 30	200 ± 30
−	200	10	0.03 ± 0.01	0.029 ± 0.006	−		nd	
−	500	10	0.04 ± 0.01	0.065 ± 0.009	−	0.04 ± 0.01	260 ± 30	210 ± 30
10	−	10	0.017 ± 0.008	0.045 ± 0.005	−		nd	

[a] nd, not determined. [b] DTT was added before the start of the experiment; BH_4 and L-arginine were added at zero time to 5 μM nNOS(BH_4−) in 50 mM triethanolamine/HCl (pH 7.0) at ambient temperature. [c] The reaction was monitored by measuring the change in the peak-to-trough absorbance difference. The absorbance changes were fitted to the equation: $\Delta\Delta A(t) = \Delta A \exp(-k_{obs}t) + \alpha t$, in which k_{obs} is the observed first-order rate constant, ΔA the corresponding absorbance change, and α, expressed in absorbance units per minute, the slope of a linear fit to the slower phase. This slower phase was not observed in the presence of high concentrations of DDT. Please note that, because of the different initial spectra, the amplitude of the absorbance changes induced by L-arginine or BH_4 in the presence of DTT cannot be directly compared to that observed in the absence of DTT. [d] Samples were taken from the absorbance cuvette at various times after BH_4 or L-arginine addition. The specific activity was determined by measuring the amount of L-citrulline produced in 2 min under standard assay conditions (see Materials and Methods). The results were fitted to the equation specific act.(t) = act.$_0$ + Δact. exp($-k_{obs}t$), in which k_{obs} is the observed first-order rate constant, Δact. the corresponding increase in activity, and act.$_0$ the activity at zero time. [e] A superior fit was obtained by fitting the results to the sum of two exponentials, with k_{obs} values of 0.4 and 0.04 min^{-1} and ΔA values of 0.0383 ± 0.0007 and 0.0651 ± 0.0005. [f] An excellent fit could also be obtained by fitting the results to the sum of two exponentials with k values of 0.4 and 0.04 min^{-1}; the resulting Δact. values were 180 ± 60 and 560 ± 60 nmol·mg^{-1}·min^{-1}, and act.$_0$ was 120 ± 40 nmol·mg^{-1}·min^{-1}.

we present here demonstrate that, after preincubation with BH_4, nNOS(BH_4−) became indistinguishable from nNOS(BH_4+). It displayed an identical elution profile in gel filtration chromatography, exhibited the same absorbance spectrum, and was equally active in L-citrulline production. This enabled us to investigate the various ways in which BH_4 has been postulated to affect nNOS (Mayer & Werner, 1995).

In agreement with prior suggestions (Mayer et al., 1991; Heinzel et al., 1992), the virtual inactivity of nNOS(BH_4−) in L-citrulline production and the strict antagonism between production of L-citrulline and H_2O_2 as a function of the BH_4 concentration unambiguously demonstrate that BH_4 is essential for coupling the oxidation of L-arginine to the reduction of O_2.

The present results also provide new evidence for structural changes in nNOS upon BH_4 binding. The different apparent radius of nNOS(BH_4−), as compared to that of nNOS(BH_4+) on the one hand, and the profoundly different heme absorbance spectrum indicate that BH_4 binding affects both the heme binding pocket and the overall protein structure.

High- and Low-Spin Heme Structures in BH_4-Deficient nNOS

The absorbance spectrum of nNOS(BH_4−) indicates a mixture of three compounds: the native high-spin form with the absorbance maximum at 398 nm, a second compound with the maximum at 418 nm, and a third one that absorbs at 456 and about 380 nm. Conversion of the last two forms into the 398 nm compound by Arg or BH_4 was accompanied by an increase of the 650 nm band, which is diagnostic for high-spin heme. On this basis, we ascribe both the 418 and 456 nm forms to low-spin compounds. The 418 nm absorbance was formerly shown to be present in a small fraction of nNOS(BH_4+) (McMillan & Masters, 1993; Pufahl & Marletta, 1993; Matsuoka et al., 1994). By comparison with cytochrome P450, it has been ascribed (Matsuoka et al., 1994) to low-spin hexacoordinate heme, with a weakly bound ligand, most likely H_2O, at the sixth coordination site (Poulos et al., 1986).

The third compound, with maxima at 456 and about 380 nm, closely resembles the bisthiolate−heme complex, observed in the presence of DTT or β-mercaptoethanol, as well as the bisthiolate complexes of cytochrome P450 (Yu et al., 1974; Sono et al., 1982), chloroperoxidase (Sono et al., 1984), and model compounds (Ruf & Wende, 1977; Ullrich et al., 1977). We propose that this enzyme form has a thiolate as a sixth heme ligand. This second thiolate is probably derived from the fairly high concentration of β-mercaptoethanol (5−6 mM) in the absorbance experiments.

The spectrum we found in the presence of DTT has been observed before with iNOS, but only after incubation in 2 M urea (Abu-Soud et al., 1995a). In that case too, it was ascribed to the formation of a hexacoordinate low-spin compound with a thiolate from DTT, which was present during the experiments at a 1 mM concentration, as the sixth ligand to the heme. Since DTT did not bind in the absence of urea and urea caused dissociation of the enzyme dimer, it was concluded that dissociation of the iNOS dimer exposed a sixth coordination site of the heme to solvent. However, since nNOS(BH_4−) is still fully dimeric as long as it contains a heme, the crucial event may be loss of BH_4 rather than dissociation of subunits (Abu-Soud et al., 1995a; Ghosh et al., 1996; Klatt et al., 1996).

Low- to High-Spin Conversion

The absorbance changes observed upon addition of Arg and/or BH_4 to nNOS(BH_4−) show that either compound can induce a conversion of the two low-spin compounds into the high-spin form that predominates in nNOS(BH_4+). From the fact that the transition rate is independent of the concentration of either compound, we conclude that a slow conformational change around the heme site governs the transition. The small absorbance changes that occurred, with the same rate, in the absence of Arg and BH_4, can be explained by a shift in the spin state equilibrium, caused by the decrease in the β-mercaptoethanol concentration upon dilution of the NOS sample.

The observation that the far slower transition rates for the DTT-preincubated enzyme were also independent of the Arg

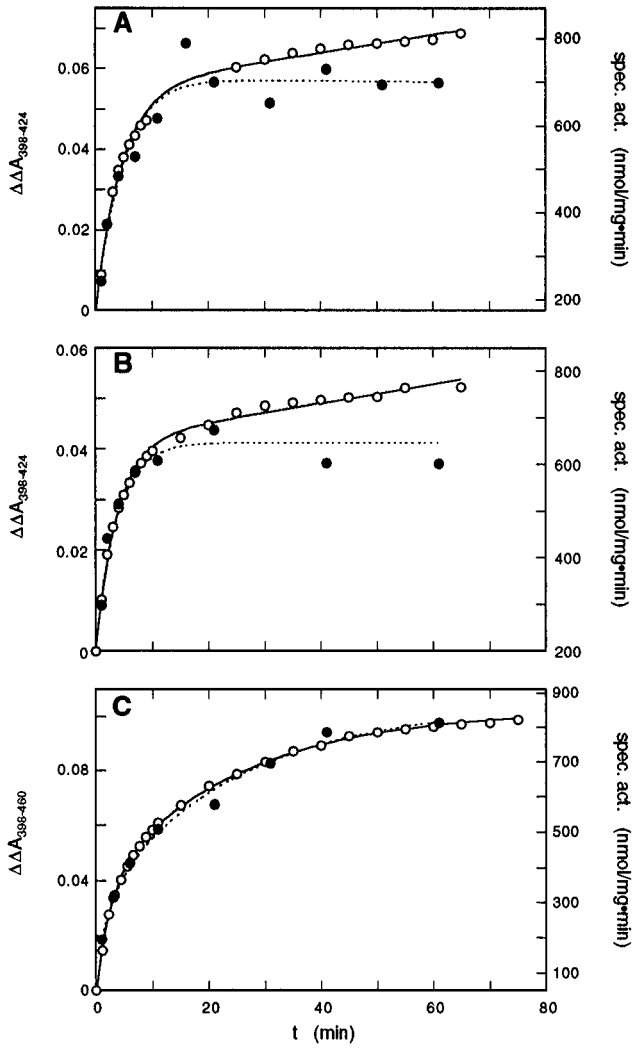

FIGURE 6: Correlation between BH_4- and Arg-induced changes in the absorbance spectrum and activity of nNOS(BH_4−). The peak-to-trough difference of the absorbance difference spectrum generated by the addition of Arg or BH_4 was measured and followed in time (open circles, continuous lines). L-Citrulline formation (closed circles, dashed lines) was determined as described in Materials and Methods. The reaction was allowed to proceed for only 2 min to minimize the effect of BH_4- and Arg-induced activation during the assay: (A) effects induced by incubation with 200 μM Arg, (B) effects induced by incubation with 10 μM BH_4, and (C) effects induced by incubation with 200 μM Arg in the presence of 1 mM DTT. Experimental conditions were as follows: 4.7 μM nNOS-(BH_4−), 50 mM triethanolamine/HCl (pH 7.0), and 25 °C. The changes in absorbance and activity in panels A and B were both fitted to the equation $y(t) = y_0 + \Delta y[1 - \exp(-kt)] + \alpha t$, in which $y(t)$ represents the observed absorbance changes and specific activities, y_0 is the apparent activity at zero time, Δy is the amplitude of the first-order changes in absorbance and activity, k is the observed first-order rate constant, and α is the slope of a linear increase in absorbance (or activity). The linear increase represents the slower phase in the absorbance changes, the first-order character of which does not become evident in the first 60 min. The data in panel C were fitted to a sum of two exponentials [$y(t) = y_0 + \Delta y_1[1 - \exp(-k_1 t)] + \Delta y_2[1 - \exp(-k_2 t)]$, with Δy_1, Δy_2, k_1, and k_2 representing the amplitudes and rate constants of the fast and slow phases, respectively]. In all panels, the lines drawn through the absorbance data are best fits to the equations; to illustrate the similarities between the absorbance and activity changes, we fitted lines through the activity data points using the same k values as obtained for the absorbance changes: 0.22 min^{-1} for panel A, 0.26 min^{-1} for panel B, and 0.40 and 0.04 min^{-1} for panel C.

or BH_4 concentration suggests that the same process determines the conversion under those conditions as well. The fact that the rate decreased with increasing DTT concentrations may be explained by assuming that the rate is now also dependent on a rapid equilibrium for the binding of DTT to the low-spin enzyme. In agreement with this assumption, the Arg-induced conversion was incomplete when the enzyme had been preincubated with high concentrations of DTT, and the amount of low-spin nNOS(BH_4−) that was converted increased with increasing Arg concentrations and decreased with increasing DTT. The results can all be accommodated in the reaction sequence shown in Scheme 1.

Scheme 1: Interconversion of High- and Low-Spin Forms of nNOS[a]

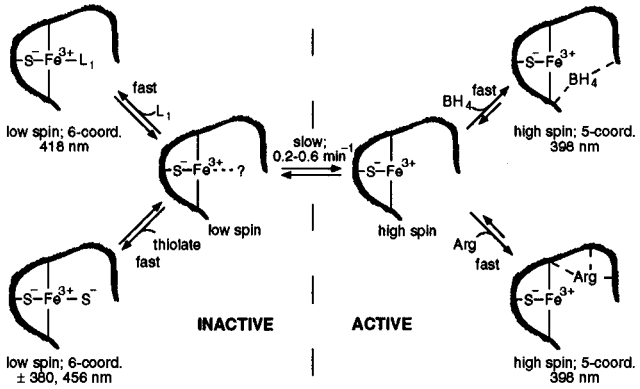

[a] The pivotal reaction is the slow (0.003−0.010 s^{-1}) conversion between both spin states. The equilibrium is affected by the subsequent binding of BH_4 and/or Arg to the 398 nm high-spin state and of ligands to the low-spin heme that produce either a compound absorbing at approximately 418 nm (imidazole; McMillan & Masters, 1993) or a compound exhibiting a hyperporphyrin spectrum with bands at 380 and 456 nm (thiolates). The presence of a weakly bound sixth ligand, such as H_2O, to the low-spin state in the absence of exogenous ligands cannot be established from the present data.

The transition of the small fraction of hexacoordinate low-spin heme, present in native nNOS, upon addition of Arg to the high-spin pentacoordinate form is well-documented (McMillan & Masters, 1993, 1995; Matsuoka et al., 1994; Gerber & Ortiz de Montillano, 1995; Roman et al., 1995) and has its counterpart in the low- to high-spin transition observed after the addition of substrate to cytochrome P450 (Schenkman et al., 1967; Dawson & Sono, 1987). However, whereas NOS is already largely high-spin in the absence of Arg, low-spin heme predominates in most cytochrome P450s. The absorbance spectrum of nNOS(BH_4−) clearly shows that this difference is caused by the presence in NOS of BH_4, and that the low- to high-spin conversion can also be accomplished by the addition of BH_4, as was already suggested by observations made with the nNOS oxygenase domain (McMillan & Masters, 1995). Our results unequivocally demonstrate that the transition actually precedes the binding of Arg and BH_4, instead of being caused by it.

Correlation between the State of the Heme and NOS Activity

In all cases, we observed a striking correlation between the fraction of enzyme present in the native high-spin 398 nm form and NOS activity. We conclude that the low-spin forms of nNOS, which absorb at 418 and 456 nm, are inactive and that a slow conformational change around the heme site is required for activation. Very similar observations with BH_4-deficient iNOS (Tzeng et al., 1995) were

ascribed to the dimerization of the enzyme that is induced by BH_4. Since BH_4-deficient nNOS is already dimeric as isolated, we conclude that either the effect of BH_4 on iNOS differs from that on nNOS or the dimerization observed after the addition of BH_4 to iNOS is induced together with activation by the same slow conformational low- to high-spin transition of the heme, which seems to be more likely.

The slow conversion of nNOS(BH_4−) into the active high-spin form must cause a substantial lag phase in the citrulline assay unless the enzyme is preincubated with either Arg or BH_4. This probably explains the relatively low activity reported for pteridine-free neuronal (List et al., 1996) and endothelial (Rodríguez-Crespo et al., 1996) NOS.

BH_4 and L-NNA Binding to nNOS

The binding of BH_4 to nNOS(BH_4+) was the subject of a previous study (Klatt et al., 1994a). The results of that study appeared fairly straightforward, allowing the determination of a second-order association rate constant (1.3×10^6 $M^{-1}\cdot min^{-1}$) and a first-order dissociation rate constant (0.32 s^{-1}), which yielded a kinetic dissociaton equilibrium constant (0.25 μM) in good agreement with a value obtained from competition experiments (0.23 μM). Yet some questions remained. Most importantly, since nNOS(BH_4+) already contains one BH_4 per dimer and no evidence was found for the binding of BH_4 with two different affinities, it remained to be established whether a second binding site (per dimer) exists and, if so, whether the observations were to be ascribed to the binding of BH_4 to the second, low-affinity site or to exchange of the BH_4 already bound at the first, high-affinity site. The availability of BH_4-free nNOS offered the unique opportunity to find answers to these questions. The results furnished the first clear evidence of BH_4 binding to a high-affinity site on nNOS.

BH_4 Binds Rapidly to Arg-Preincubated nNOS(BH_4−). Paramount among the results is the observation of very fast BH_4 association (within the first 20 s) in the presence of Arg to nNOS(BH_4−) but not to nNOS(BH_4+). This clearly demonstrates that BH_4 binding to the high-affinity site of NOS, *i.e.* to a BH_4-free dimer that has been transformed into the proper, high-spin conformation by preincubation with Arg, is fast (Scheme 2, reaction C). Some fast BH_4 binding was also observed with nNOS(BH_4+). This is easily explained by the fact that usually the BH_4:heme ratio in nNOS(BH_4+) varies between 0.40 and 0.45; *i.e.* 10−20% of the enzyme contains no BH_4. As was to be expected on the basis of the spectral studies reported above, little fast binding occurred unless the enzyme was preincubated with Arg, since otherwise, the BH_4 association rate cannot exceed the slow conformational change that has to precede BH_4 binding (Scheme 2, reaction A).

There Is Strong Cooperativity between Substrate and BH_4 Binding. A second major result, the observation that preincubation of nNOS(BH_4+) with BH_4 causes a 2-fold increase of the concentration of bound L-NNA, suggests that only in the presence of excess BH_4 will nNOS bind two L-NNA molecules per dimer, whereas nNOS(BH_4+), which contains one BH_4 per dimer, binds just 1 equiv of L-NNA. This implies the presence of two identical L-NNA binding sites per dimer, the affinity of which is greatly enhanced by BH_4. Consequently, this result also offers strong evidence for the existence of a second, low-affinity binding site for

Scheme 2: Binding of Tetrahydrobiopterin and L-Arginine to Dimeric nNOS[a]

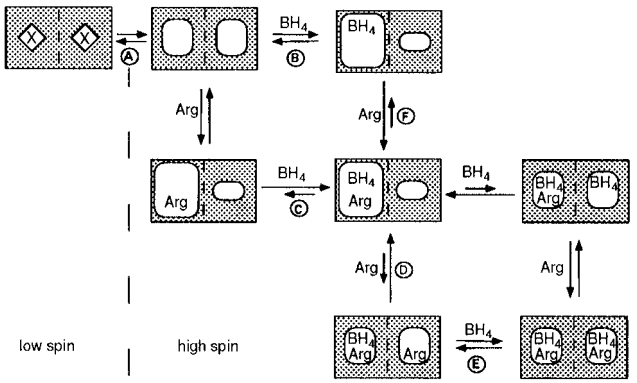

[a] Reaction A is the slow conformational change accompanying the spin transition of the NOS heme ($k_{forward}$ = 0.2−0.6 min^{-1}). This reaction, followed by comparatively fast reaction B, may be responsible for the slow, low-yield, and zero-order binding of BH_4 to nNOS(BH_4−) without Arg. After preincubation with Arg, the rapid, high-yield reaction C occurs ($k_{on} \geq 10^8$ $M^{-1}\cdot min^{-1}$). The slow, low-yield, zero-order reaction with nNOS(BH_4+) may be due to the exchange of the endogenous unlabeled BH_4 by the radioligand, represented by the reverse and forward reactions B (k_{off} = 0.3 min^{-1}; K_d = 250 nM; k_{on} = 1.2×10^6 $M^{-1}\cdot min^{-1}$). The slow, high-yield, zero-order, and BH_4 concentration-independent association of BH_4 to nNOS(BH_4+) in the presence of Arg can be explained if the slow association of Arg (reaction D) is followed by the fast association of BH_4 (reaction E, k_{off} = 0.07 min^{-1}, K_d = 37 nM, k_{on} = 1.9×10^6 $M^{-1}\cdot min^{-1}$). In the absence of exogenous BH_4, catalysis is expected to involve only reaction F and, for very low Arg concentrations and very dilute enzyme and thus very low BH_4 concentrations, possibly reactions A and B as well. In the presence of BH_4, catalysis will involve reactions F and, particularly at high Arg and BH_4 levels, reactions D and E (or the corresponding pair of reactions that has BH_4 binding first). Because of the strong cooperativity between Arg and BH_4 binding, and the strong anticooperativity between the binding of two BH_4 molecules, the enzyme states $NOS_2\cdot(BH_4)_2\cdot$Arg and $NOS_2\cdot BH_4\cdot Arg_2$ will not accumulate, and transition between $NOS_2\cdot BH_4\cdot$Arg and $NOS_2\cdot(BH_4)_2\cdot Arg_2$ will proceed as the one-step concerted association/dissociation of BH_4 and L-arginine/L-citrulline.

BH_4 on nNOS, in good agreement with the fact that excess BH_4 stimulates the L-citrulline-producing activity of nNOS 2-fold (Baek et al., 1993; Roman et al., 1995; List et al., 1996). The lack of L-NNA binding to nNOS(BH_4−), which is in agreement with a previous report (Roman et al., 1995), further corroborates our conclusions. Since the binding rate of L-NNA was found to be linearly dependent on the L-NNA concentration, the estimation of a second-order association rate constant and of an equilibrium dissociation constant was possible. We obtained values for L-NNA binding to nNOS(BH_4+) in the presence of BH_4 of $(2.7 \pm 0.5) \times 10^4$ $M^{-1}\cdot s^{-1}$ for k_{on}, $(1.32 \pm 0.07) \times 10^{-3}$ s^{-1} for k_{off}, and 50 ± 10 nM for K_d and similar values for the other experimental conditions (Table 2). These values are in fair agreement with those previously reported (Klatt et al., 1994a,b; Roman et al., 1995).

BH_4-Independent Reactions Govern the Rate of Slow BH_4 Binding. Whereas the association of L-NNA could be well fitted by a simple pseudo-first-order approximation, this was clearly not the case with BH_4 binding. The latter reaction did not depend on the concentration of BH_4, at least in the case of nNOS(BH_4+) after preincubation with Arg. As a consequence, since the enzyme concentration (187.5 nM) was much higher than the radioligand concentration (7.0−9.2 nM), pseudo-zero-order reactions were observed. Therefore, the observed binding rates cannot be attributed to the actual

association of BH_4. Values for the apparent association rate constants can, however, be estimated from the previously determined K_d values (Klatt et al., 1994a) and the k_{off} values derived from the present studies. Both nNOS(BH_4+) and nNOS(BH_4−) yielded k_{off} values of $(1.13 \pm 0.05) \times 10^{-3}$ and $(4 \pm 1) \times 10^{-3}$ s^{-1} in the presence and absence of Arg, respectively (Table 1). With the corresponding values for K_d of 37 and 230 nM (Klatt et al., 1994a), one arrives at association rate constants of 3.1×10^4 and 1.7×10^4 $M^{-1}\cdot s^{-1}$. It should be noted that these values, both with and without Arg, represent low-affinity binding modes of BH_4 (Scheme 2, equilibria E and B). The high-affinity association rate constant for binding of the first equivalent of BH_4 after preincubation with Arg must be 1×10^6 $M^{-1}\cdot s^{-1}$ or higher (Scheme 2, reaction C). This puts an upper limit on the corresponding K_d of 1 nM.

The identity of the BH_4-independent reaction step that gives rise to the zero-order kinetics cannot be determined on the basis of the present data and may not be the same in the presence and absence of Arg and endogenous BH_4. In the case of nNOS(BH_4−) in the absence of Arg, the slow spin transition, which was observed in the optical experiments, may be involved (Scheme 2, reaction A). For nNOS(BH_4+) in the absence of Arg, the affinity of the enzyme for binding a second BH_4 molecule may be so low that the reaction proceeds via the unliganded enzyme after dissociation of the unlabeled BH_4. According to this model, in the absence of Arg, only one molecule of BH_4 would be bound to nNOS with a K_d on the order of 10^{-7} M (Scheme 2, reverse and forward reactions B). In the presence of Arg, a slow reaction might arise, if the slow binding of a second Arg molecule to a nNOS dimer is followed by the cooperative rapid binding of a second molecule of BH_4 (Scheme 2, reactions D and E). This second BH_4 molecule would, according to the model, display an apparent affinity on the order of 10^{-8} M, in reality representing the combined binding of BH_4 and Arg.

nNOS Dimers Accommodate Two Identical but Strongly Anticooperative BH_4 Binding Sites. From the dissociation experiments, two conclusions can be drawn. The rate of dissociation only depended on whether Arg was present, which demonstrates that BH_4 addition to nNOS(BH_4+) and nNOS(BH_4−) eventually generates the same compound. More importantly, all radioligand was removed in the presence of excess unlabeled ligand; even the rapid binding of BH_4 to nNOS(BH_4−) was reversed. Since this reaction essentially produces nNOS(BH_4+), with 1 equiv of BH_4 bound per dimer with high affinity, this implies that, contrary to earlier observations, exchange of the high-affinity bound pteridine does occur (Scheme 2, reverse reaction B). The observation that BH_4 dissociation from nNOS(BH_4−) in the presence of Arg, conditions under which radioligand is expected to be bound at both high- and low-affinity sites, was complete and monophasic clearly shows that both sites are identical and that low-affinity binding arises from anticooperativity between the two sites. The model shown in Scheme 2 adequately explains most of our observations.

General Discussion and Conclusions

As already mentioned, one distinction between NOS and cytochrome P450 is that, whereas the heme in nNOS(BH_4+) is mostly five-coordinate high-spin as isolated, most cytochrome P450s contain a six-coordinate low-spin heme that is converted into the five-coordinate high-spin form only in the presence of substrate (Dawson & Sono, 1987). Our results demonstrate that this difference can be ascribed to the fact that, unlike cytochrome P450, NOS contains BH_4 as a tightly bound cofactor. Although the significance of this spectroscopic distinction cannot be established on the basis of the present data, one consequence might be that the shift in the equilibrium toward a five-coordinated form, which is induced by BH_4, aids in expelling NO from the active site cavity. Like many hemoproteins, cytochrome P450 binds NO with high affinity (O'Keeffe et al., 1978; Dawson & Sono, 1987; Nakano et al., 1996). Likewise, NOS has been shown to form both ferric and ferrous complexes with NO (Wang et al., 1994; Hurshman & Marletta, 1995), which could give rise to product inhibition. Indeed, it has been reported that during catalysis most of the NOS heme is present as an inhibitory nitrosyl complex (Abu-Soud et al., 1995b). Conceivably, BH_4 stimulates NO dissociation by lowering the affinity of the heme for binding a sixth ligand.

Doubtless, BH_4 is also an allosteric effector of substrate binding. In agreement with previous studies (Klatt et al., 1994a; Roman et al., 1995), we observed strong cooperativity between BH_4 and Arg or L-NNA binding, although the underlying mechanism appears to be more complex than expected. Certainly, simple sets of association/dissociation equilibria do not suffice to describe the interactions. Nevertheless, the basic concept of the potential regulation of the substrate affinity by BH_4 is confirmed.

In addition to, or concurrent with, these allosteric effects on substrate binding, BH_4 engenders substantial, though ill-defined, changes in the structure of NOS. For iNOS, these changes were associated with the catalytically obligatory formation of a dimer (Abu-Soud et al., 1995a; Tzeng et al., 1995; Ghosh et al., 1996). Although in the case of nNOS exogenous BH_4 brings about the formation of an extremely stable, SDS-resistant dimer, nNOS dimers are formed without BH_4, and the presence of heme seems to be the only prerequisite for dimerization (Klatt et al., 1995, 1996). Moreover, experiments with dimers, consisting of one active and one inactive monomer, demonstrated that the activity of one half of the dimer was unaltered by the inactivity of the other half (Siddhanta et al., 1996). Therefore, it remains to be established whether the proposed relationship between enzyme quaternary structure and catalytic activity (Baek et al., 1993; Abu-Soud et al., 1995a; Ghosh & Stuehr, 1995; Tzeng et al., 1995; Ghosh et al., 1996) is real or if both dimerization and enzyme activation are rather the result of the same structural changes. Notably, dimerization of BH_4-free eNOS was reported to be unaffected by BH_4 (Rodríguez-Crespo et al., 1996). Nevertheless, the anticooperativity between the two BH_4 binding sites per dimer that we postulate does provide a means of fine tuning the regulatory role of BH_4 in catalysis. As discussed previously (Mayer & Werner, 1995), this regulation may not target the NO formation rate as such but rather the relative rates of nitric oxide and superoxide production. The present results suggest that at high Arg/BH_4 concentrations nNOS will produce NO, whereas at low Arg/BH_4 concentrations, the simultaneous formation of O_2^- and NO will mainly yield $ONOO^-$.

In summary, we demonstated (1) a strict correlation between the presence of BH_4 and the coupling of reductive

oxygen activation to Arg oxidation; (2) profound structural changes induced by the presence of one BH_4 molecule per dimer but little further effect upon complete saturation with BH_4; (3) a slow equilibrium for NOS heme between two inactive low-spin states and the active high-spin state, the position of which is shifted toward the native form by BH_4 and/or Arg and in the opposite direction by thiolates; (4) the rapid association of BH_4 to a high-affinity binding site on Arg-preincubated nNOS(BH_4−), which is occupied in nNOS(BH_4+); (5) the monophasic and complete exchange of enzyme-bound BH_4 by free BH_4 and thus the existence of two identical, but highly anticooperative pteridine binding sites per dimer; (6) slow, zero-order, concentration-independent binding of BH_4 to NOS in the absence of Arg, indicative of slow enzyme conformational changes and/or slow dissociation of endogenous BH_4; and (7) a 2-fold increase in L-NNA binding in the presence of excess BH_4, suggesting the existence of two identical substrate binding sites, as well as two BH_4 binding sites per dimer. The model we put forward incorporates most of these observations but requires further corroboration.

REFERENCES

Abu-Soud, H. M., Loftus, M., & Stuehr, D. J. (1995a) *Biochemistry 34*, 11167−11175.

Abu-Soud, H. M., Wang, J., Rousseau, D. L., Fukuto, J. M., Ignarro, L. J., & Stuehr, D. J. (1995b) *J. Biol. Chem. 270*, 22997−23006.

Baek, K. J., Thiel, B. A., Lucas, S., & Stuehr, D. J. (1993) *J. Biol. Chem. 268*, 21120−21129.

Bradford, M. M. (1976) *Anal. Biochem. 72*, 248−254.

Dawson, J. H., & Sono, M. (1987) *Chem. Rev. 87*, 1255−1276.

Degtyarenko, K. N., & Archakov, A. I. (1993) *FEBS Lett. 332*, 1−8.

Fulco, A. J. (1991) *Annu. Rev. Pharmacol. Toxicol. 31*, 177−203.

Gerber, N. C., & Ortiz de Montellano, P. R. (1995) *J. Biol. Chem. 270*, 17791−17796.

Ghosh, D. K., & Stuehr, D. J. (1995) *Biochemistry 34*, 801−807.

Ghosh, D. K., Abu-Soud, H. M., & Stuehr, D. J. (1996) *Biochemistry 35*, 1444−1449.

Griffith, O. W., & Stuehr, D. J. (1995) *Annu. Rev. Physiol. 57*, 707−736.

Harteneck, C., Klatt, P., Schmidt, K., & Mayer, B. (1994) *Biochem. J. 304*, 683−686.

Heinzel, B., John, M., Klatt, P., Böhme, E., & Mayer, B. (1992) *Biochem. J. 281*, 627−630.

Hurshman, A. R., & Marletta, M. A. (1995) *Biochemistry 34*, 5627−5634.

Kaufman, S. (1993) *Annu. Rev. Nutr. 13*, 261−286.

Klatt, P., Schmidt, K., Uray, G., & Mayer, B. (1993) *J. Biol. Chem. 268*, 14781−14787.

Klatt, P., Schmid, M., Leopold, E., Schmidt, K., Werner, E. R., & Mayer, B. (1994a) *J. Biol. Chem. 269*, 13861−13866.

Klatt, P., Schmidt, K., Brunner, F., & Mayer, B. (1994b) *J. Biol. Chem. 269*, 1674−1680.

Klatt, P., Schmidt, K., Lehner, D., Glatter, O., Bächinger, H. P., & Mayer, B. (1995) *EMBO J. 14*, 3687−3695.

Klatt, P., Pfeiffer, S., List, B. M., Lehner, D., Glatter, O., Bächinger, H. P., Werner, E. R., Schmidt, K., & Mayer, B. (1996) *J. Biol. Chem. 271*, 7336−7342.

List, B. M., Klatt, P., Werner, E. R., Schmidt, K., & Mayer, B. (1996) *Biochem. J. 315*, 57−63.

Marletta, M. A. (1993) *J. Biol. Chem. 268*, 12231−12234.

Masters, B. S. S. (1994) *Annu. Rev. Nutr. 14*, 131−145.

Matsuoka, A., Stuehr, D. J., Olson, J. S., Clark, P., & Ikeda-Saito, M. (1994) *J. Biol. Chem. 269*, 20335−20339.

Mayer, B. (1995) in *Nitric Oxide in the Nervous System* (Vincent, S. R., Ed.) pp 21−42, Academic Press, New York.

Mayer, B., & Werner, E. R. (1995) *Naunyn-Schmiedebergs Arch. Pharmacol. 351*, 453−463.

Mayer, B., John, M., Heinzel, B., Werner, E. R., Wachter, H., Schultz, G., & Böhme, E. (1991) *FEBS Lett. 288*, 187−191.

Mayer, B., Klatt, P., Werner, E. R., & Schmidt, K. (1994) *Neuropharmacology 33*, 1253−1259.

Mayer, B., Klatt, P., Harteneck, C., List, B. M., Werner, E. R., & Schmidt, K. (1996) *Methods Neurosci. 31*, 130−139.

McMillan, K., & Masters, B. S. S. (1993) *Biochemistry 32*, 9875−9880.

McMillan, K., & Masters, B. S. S. (1995) *Biochemistry 34*, 3686−3693.

Moncada, S., Palmer, R. M. J., & Higgs, E. A. (1991) *Pharmacol. Rev. 43*, 109−142.

Nakano, R., Sato, H., Watanabe, A., Ito, O., & Shimizu, T. (1996) *J. Biol. Chem. 271*, 8570−8574.

O'Keeffe, D. H., Ebel, R. E., & Peterson, J. A. (1978) *J. Biol. Chem. 253*, 3509−3516.

Poulos, T. L., Finzel, B. C., & Howard, A. J. (1986) *Biochemistry 25*, 5314−5322.

Pufahl, R. A., & Marletta, M. A. (1993) *Biochem. Biophys. Res. Commun. 193*, 963−970.

Rodríguez-Crespo, I., Gerber, N. C., & Ortiz de Montellano, P. R. (1996) *J. Biol. Chem. 271*, 11462−11467.

Roman, L. J., Sheta, E. A., Martasek, P., Gross, S. S., Liu, Q., & Masters, B. S. S. (1995) *Proc. Natl. Acad. Sci. U.S.A. 92*, 8428−8432.

Ruf, H. H., & Wende, P. (1977) *J. Am. Chem. Soc. 99*, 5499−5500.

Schenkman, J. B., Remmer, H., & Estabrook, R. W. (1967) *Mol. Pharmacol. 3*, 113−123.

Siddhanta, U., Wu, C., Abu-Soud, H. M., Zhang, J., Ghosh, D. K., & Stuehr, D. J. (1996) *J. Biol. Chem. 271*, 7309−7312.

Sono, M., Andersson, L. A., & Dawson, J. H. (1982) *J. Biol. Chem. 257*, 8308−8320.

Sono, M., Dawson, J. H., & Hager, L. P. (1984) *J. Biol. Chem. 259*, 13209−13216.

Tzeng, E., Billiar, T. R., Robbins, P. D., Loftus, M., & Stuehr, D. J. (1995) *Proc. Natl. Acad. Sci. U.S.A. 92*, 11771−11775.

Ullrich, V., Ruf, H. H., & Wende, P. (1977) *Croat. Chem. Acta 49*, 213−222.

Wang, J., Rousseau, D. L., Abu-Soud, H. M., & Stuehr, D. J. (1994) *Proc. Natl. Acad. Sci. U.S.A. 91*, 10512−10516.

Werner, E. R., Schmid, M., Werner-Felmayer, G., Mayer, B., & Wachter, H. (1994) *Biochem. J. 304*, 189−193.

Witteveen, C. F. B., Giovanelli, J., & Kaufman, S. (1996) *J. Biol. Chem. 271*, 4143−4147.

Yu, C.-A., Gunsalus, I. C., Katagiri, M., Suhara, K., & Takemori, S. (1974) *J. Biol. Chem. 249*, 94−101.

BI961931J